A Reaction Pathway for Nanoparticle Formation in Rich Premixed Flames

A. D'ANNA,* A. VIOLI, and A. D'ALESSIO
Dipartimento di Ingegneria Chimica, Università di Napoli "Federico II" Napoli, Italy

and

A. F. SAROFIM
Department of Chemical and Fuels Engineering, University of Utah, Salt Lake City, Utah, USA

Aromatics growth beyond 2-, 3-ring PAH is analyzed through a radical-molecule reaction mechanism which, in combination with a previously developed PAH model, is able to predict the size distribution of aromatic structures formed in rich premixed flames of ethylene at atmospheric pressure with C/O ratios across the soot threshold limit. Modeling results are in good agreement with experimental data and are used to interpret the ultraviolet absorption and the light scattering measured in flames before soot inception. The model shows that the total number concentration of high molecular mass aromatics and the different moments of the size distribution are functions of both the PAH and H-atom concentrations, two quantities which have different trends as functions of the residence time and the C/O ratio. Regimes of nearly stoichiometric or slightly rich premixed combustion are dominated by reactions between aromatics which lead to the formation of particles with sizes of the order of 3 to 4 nm. At higher C/O ratios the formation of nanoparticles is less efficient. Particles with sizes of the order of 2 nm are predicted in flames at the threshold of soot formation, whereas particles with sizes around 1 to 1.5 nm are predicted in fully sooting conditions.

INTRODUCTION

Epidemiological studies have demonstrated that particulate matter, even at the low concentrations allowed by modern technologies, has an impact on human health [1–3]. The toxicological mechanisms are still unclear. There are strong indications that particle surface area is more important than particle mass in determining the effects of air pollution: particles that are non-toxic when inhaled as aggregates in the micrometer-sized range, can be toxic when inhaled as single particles in the nanometer-sized range [4, 5].

A significant amount of anthropogenic particles are emitted from engines and stationary combustion sources in form of nanoparticles. Consequently, there is a great scientific and practical interest in the study of their formation and their evolution in the environment [5, 6]. Many investigations have been focused on the study of the formation and oxidation of soot particles (typical sizes larger than 20 nm) whereas less effort has been concentrated on carbonaceous nanoparticles with smaller sizes down to 5 nm. Nanoparticles have been detected downstream of the flame front in rich premixed flames [7–9], during acetylene pyrolysis behind shock waves [10], on the axis of co-flow diffusion flames [11], and recently at the exhausts of gasoline and diesel engines [12, 13].

The spectroscopic characterizations of premixed flames have shown that these particles are initially transparent to visible radiation and exhibit spectroscopic properties typical of PAHs with few condensed aromatic rings [8, 14]. These compounds are formed at a high rate in rich flames just downstream of the flame front and their concentration accounts for the total amount of soot formed in slightly sooting conditions [15–17]. Light scattering measurements have shown that they build-up rapidly to nano-sized particles and their dimension remains constant up to the inception of soot. At this point, coagulation starts, the scattering signal increases by orders of magnitude and larger particles are formed [8, 14, 15].

The formation of particulate matter in rich combustion is typically modeled through the formation of benzene molecules that grow to high molecular mass aromatics including PAH. The larger PAH compounds coagulate to form the first soot nuclei and finally these nuclei grow

* Corresponding author. E-mail: danna@irc.na.cnr.it

COMBUSTION AND FLAME 127:1995–2003 (2001)

Published by Elsevier Science Inc.

0010-2180/01/$–see front matter
PII S0010-2180(01)00303-0

by surface reactions that add carbon from the gas phase [18–20]. The growth of aromatics from benzene is modeled by using the alternating H abstraction acetylene addition (HACA) route. Larger PAHs can be modeled using moments of the PAH distribution function in which the kinetics of an infinite sequence of polymerization-type reactions based on the HACA mechanism is described by a small number of differential equations [18].

Reactions involving resonantly stabilized radicals have been proposed for modeling the fast formation of aromatics in addition to the classical HACA route [21, 22]. This class of reactions to form 2-, 3-ring PAHs can be used to simulate the experimental evidence of a fast formation rate of aromatic compounds and their total concentration in slightly sooting ethylene flames in a wide range of temperatures and C/O ratios [23–25]. The same kinetic model has been recently employed to interpret the ultraviolet absorption measurements in rich flames across the soot threshold limit [17]. The model correctly predicts the volume fraction of aromatic compounds responsible for ultraviolet absorption but it does not describe the detailed growth routes for the formation of high molecular mass aromatics which are responsible for the scattering signal measured in flames before soot inception [15, 26].

The purpose of this paper is to present a reaction pathway which, as an extension to the previous PAH formation model, predicts the size distribution of the aromatic structures formed in flames before soot inception. The computed scattering of high molecular mass aromatics is compared with the scattering signal measured in flame from which the contribution of gaseous compounds up to benzene has been subtracted. Atmospheric pressure, rich premixed flames of ethylene/air and ethylene/oxygen at different C/O ratios, above and below the soot threshold limit, are analyzed [15, 26].

MODEL DEVELOPMENT

Prediction of the growth of aromatics requires an accurate description of the main flame structure in terms of stable species and major radicals. We have previously developed and tested a kinetic model for different hydrocarbons over a wide range of operating conditions [23–25]. The agreement between the model results and the experimental data was satisfactory for both major radical species and stable intermediate compounds. The kinetic mechanism ended-up with the formation of PAH up to 2-, 3-rings and assumed that these were converted to high molecular mass structures by a fast growth process. This paper provides a reaction pathway for the growth of PAHs with a brief reference to the gas phase chemistry. A more detailed presentation of the gas phase analysis is described elsewhere [23–25]. The complete detailed reaction mechanism consists of 340 reactions and 90 chemical species.

Gas-phase Chemistry

The gas-phase mechanism includes the pyrolysis and oxidation of C1 and C2 species, the formation of benzene and further reactions leading to aromatic compounds with up to 3-rings. The formation and growth of aromatic compounds up to 3-rings, as identified by detailed chemical kinetic modeling, occurs more through the combination of resonantly stabilized radicals than through a multi-step process of acetylene addition.

The major routes of the first aromatic ring formation are propargyl self-combination

$$H_2CCCH + H_2CCCH \rightarrow C_6H_5 + H$$

and the addition of propargyl to 1-methylallenyl with the formation of benzyl radicals and their decomposition to benzene:

$$CH_3CCCH_2 + H_2CCCH$$

$$\rightarrow C_6H_5CH_2 \text{ (benzyl)} + H$$

$$C_6H_5CH_2 + H \rightarrow C_6H_5CH_3$$

$$C_6H_5CH_3 + H \rightarrow C_6H_6 + CH_3$$

The combination of cyclopentadienyl-like radicals is the controlling step of aromatic growth:

$$c\text{-}C_5H_5 + c\text{-}C_5H_5 \rightarrow C_{10}H_8 + H + H$$

$$\text{indenyl} + c\text{-}C_5H_5 \rightarrow \text{phenanthrene} + H + H$$

for some conditions greatly surpassing the HACA mechanism involving replicating H-atom abstrac-

tion from an aromatic molecule followed by acetylene addition. According to this mechanism, aromatics are rapidly formed in the main flame region and they grow up to 2-, 3-rings attaining a concentration level in flames that is comparable to the total concentration of PAHs and carbonaceous nanoparticles [23].

Growth of Aromatics Beyond 2-, 3-Ring PAHs

The growth of aromatics is modeled by a radical-molecule sequence of reactions involving five-membered ring PAHs which are present at large concentrations in the PAH inventory [27, 28]. These compounds are exceptional intermediates as they grow rapidly forming resonantly stabilized radical intermediates [29].

Aromatic compounds evaluated with the gas-phase chemistry simulations are considered as units in a molecular weight grow process based on the following reaction scheme:

$$A_i + \mathrm{H} \Leftrightarrow R_i + \mathrm{H}_2 \tag{1}$$

$$R_i + A_k \Rightarrow R_{i+k} \tag{2}$$

$$R_i + R_k \Leftrightarrow A_{i+k} \tag{3}$$

$$R_i + \mathrm{H} \Leftrightarrow A_i \tag{4}$$

where A_i is a species constituted by i gas-phase aromatic units and R_i the corresponding radical.

Reaction 1 activates the aromatic structures by H-atom abstraction. The reaction is reversible, and the forward reaction rate is assumed to be equal to 2.5E14*exp(−16000/RT) per each gas-phase PAH unit (mol, cm^3, s, cal). This value is multiplied by i in the case of species having i units inside the structure, because the H-abstraction is a function of the available number of H-atoms. The reverse reaction rate for $i = 1$ and 2 has been evaluated from the equilibrium constants. For larger values of i it was hard to have memory of the chemical structure of the species involved and hence to evaluate the equilibrium constant of the Reaction 1. The reverse reaction rate was hence kept equal to that evaluated for $i = 2$. A more accurate evaluation of the reverse reaction rates is necessary and it will require the estimation of the thermodynamic properties of larger intermediates involved in the growth process.

The radical-molecule growth reaction ($Rx2$) has been fictitious considered irreversible because of the great stability of the intermediate compounds which results in a lower reverse rate. Discussion of the nature of these intermediates is reported below. The forward reaction rate is assumed to have a collision efficiency of 0.1.

Termination occurs primarily by two mechanisms: the first one is the addition (coupling) of two growing radical intermediates, R_i and R_k, forming a stable species ($Rx3$). The rate of this reaction is assumed to be 1E12 $cm^3\ mol^{-1}\ s^{-1}$, and has been evaluated by analogy with gas-phase recombination reactions [22]. The second mechanism involves the H-atom addition to a radical ($Rx4$). The starting value for this reaction rate is taken by analogy with a typical reaction between aromatic radicals and H-atoms (i.e., $C_{10}H_7 + H$). Reaction 4 is approximated by a reversible reaction having a reverse rate constant that decreases by one order of magnitude as the molecular weight of the structure increases up to the maximum allowable value in the scheme (about 3E4 amu). This hypothesis was possible in light of the greater stability of the aromatic radicals for increasing molecular weights [30] and checked by evaluating from thermodynamic data the reverse rate of $Rx4$ for different values of $i = 1, 2$.

A schematic view of this reaction pathway is shown in Fig. 1. It was drawn considering that the PAH inventory in a flame is essentially composed by naphthalene and acenaphthylene, at least in the range of C/O ratios analyzed in the present work [28].

Computational Procedure

Computer simulations have indicated that aromatic production constitutes only a minor flux compared to the rates of the main chain reactions in the system. This result decouples the kinetics of these processes because the mass balances of H, H_2, and other radicals are not affected by the consumption and production rates of these species. In other words, aromatic growth beyond 2-, 3-rings takes place in the environment created by other reactions. This approximation will be valid at low concentrations of particulate matter.

The calculations were performed in two stages. The gas-phase chemistry was calculated

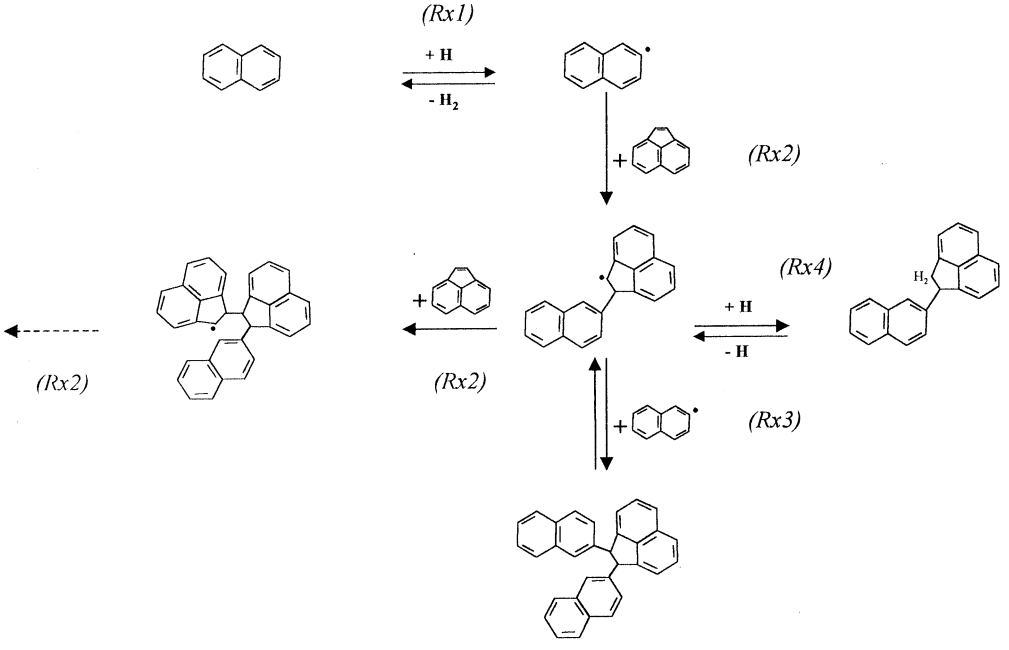

Fig. 1. A schematic diagram illustrating the mechanism of aromatic growth.

with the SANDIA burner code [31] using temperature profiles and the mass flow rates as input parameters. Then, the computed profiles of H, H_2, and total aromatics along with the temperature profile were used as input for the evaluation of the growth process.

RESULTS

Simulations were performed for two ethylene/air flames at atmospheric pressure, having C/O = 0.51 and C/O = 0.77, corresponding to non-sooting and slightly sooting conditions, respectively [26], and for different ethylene/oxygen flames with C/O ranging from nearly stoichiometric to soot forming conditions [14]. The flames were experimentally characterized by temperature profile measurements, scattering and extinction measurements in the UV and visible and UV laser induced fluorescence.

Figure 2 reports the predicted molecular mass distribution spectra of the aromatics, that is, the mass fraction dm of aromatics with molecular mass between W and $W + dW$ as a function of the molecular mass W for the slightly sooting flame (C/O = 0.77) at 1, 2, and 4 mm above the burner. The lowest height corresponds roughly to the flame front: the species formed are mainly PAHs up to 400 amu with a mass center of about 150 amu, which corresponds to the non-reacted PAHs predicted by the gas-phase model. The mass peak centered at about 2000 amu does not contribute significantly to the total amount of aromatics showing that the molecular weight growth process becomes appreciable only at higher heights. At 2 mm above the burner, the 2- and 3-ring PAHs (<200 amu) contribution decreases and the second peak broadens at 5000 amu which corresponds to particles of about 2.5 nm (based

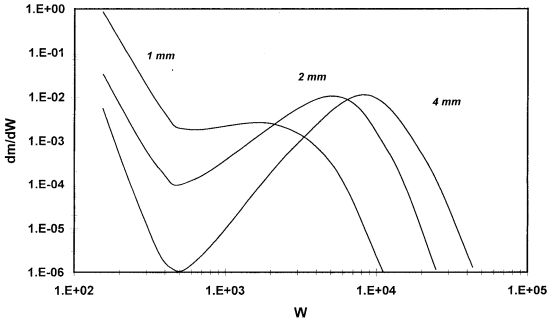

Fig. 2. Molecular mass distribution (dm/dW) spectra at 1, 2, and 4 mm above the burner in a slightly sooting ethylene/air flame with C/O = 0.77.

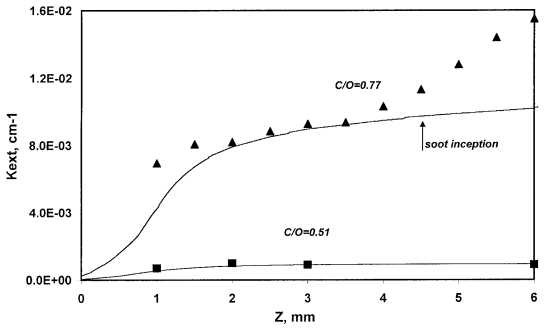

Fig. 3. Comparison between experimental (symbols) [26] and computed extinction profiles at 266 nm along the axis of rich ethylene/air flames with C/O = 0.51 and 0.77.

on the hypotheses of spherical particles with a density of 1 g/cm^3). The molecular mass of these nanoparticles at 4 mm shifts toward higher masses of 9000 amu (a size of about 3.1 nm). These results are in qualitative agreement with the molecular mass spectra of ions obtained by Homann in fuel-rich low-pressure acetylene flames [32].

Figure 3 reports the ultraviolet absorption at 266 nm predicted by the model as a function of the height above burner for the two ethylene/air flames (C/O = 0.51 and 0.77) compared with the experimental data. The modeled results have been obtained considering that the total absorption coefficient of the high molecular mass aromatics is given by the sum of the absorption coefficients of the precursor molecules. This assumption is possible since aromatic subunits in the larger structure do not interact with each other. This model is in agreement with previous spectroscopic characterization of the high molecular mass aromatics which have shown that these compounds are structures with 2-, 3-ring PAH subunits which behave spectroscopically as single non-interacting compounds. A constant molar absorption coefficient ϵ of 5000 cm^{-1}/mol/l, typical of 2-, 3-ring PAH, is used for the absorption coefficient of the aromatic subunits [17]. The agreement of model predictions with experimental data is quite good just downstream of the flame fronts of both flames, which are located at about 1 mm above the burner. The experimental absorption profile for a slightly sooting flame with C/O of 0.77 shows a fast increase in the main oxidation zone of the flame up to 2 mm; after a plateau, a second strong increase of the absorption coefficient in the post flame region is observed. This second increase starts in correspondence of the formation of soot particles which occurs at about 4 mm. The model is able to reproduce both the amount of absorbed light and also its initial fast increase. It is worth noting that the model reproduces the increase of more than one order of magnitude in the extinction coefficient as the C/O ratio is increased from 0.51 to 0.77. However, in the soot-forming zone ($z > 4$ mm) of the slightly sooting (C/O = 0.77) flame the model predictions are lower than the experimental data. The disagreement may be related to the hypothesis of non-interacting aromatic subunits which fails in the soot inception region (about 4 mm) where probably the high molecular mass aromatics undergo strong chemical changes, primarily dehydrogenation by H-atom abstraction and thermal carbonization, before their transformation to soot particles.

The light scattered by an aerosol strongly depends both on concentration and size of the scattering entities and hence the comparison of the model predictions with the scattering attributed to aromatics measured in flames is a good test of the validity of the aromatic growth mechanism. To estimate the scattering cross section for aromatic species, a group additivity rule has been considered. The molar refractivity of hydrocarbons is controlled mainly by the atoms present without regard to the chemical state [33, 34]. By using this approach, we estimate the molar refractivity of high molecular mass aromatics as the sum of the molar refractivity of 2-, 3-ring PAH subunits. Converting the molar refractivity into the index of refraction n it is possible to estimate the scattering cross section of the nanoparticles at a fixed wavelength of the incident light (266 nm in the measurements). Figure 4 shows the comparison between the measured and predicted scattering of aromatics for the two flames. The agreement of the model results with experiments is quite good (within a factor of two) for the non-sooting flame except for the data at the flame front which may be affected by the strong contribution of gaseous compounds and/or to a poor estimation of the flame temperature front. Also in the slightly sooting flame the model reproduces quite well the experimental scatter-

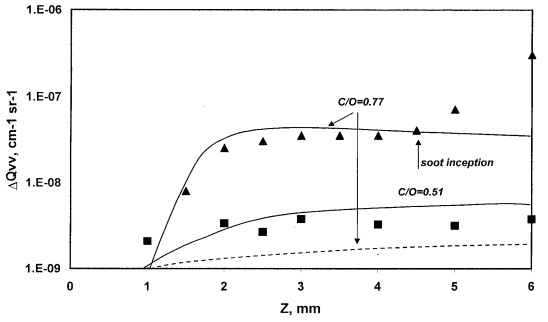

Fig. 4. Comparison between experimental (symbols) [26] and computed scattering attributed to aromatics along the axis of rich ethylene/air flames with C/O = 0.51 and 0.77.

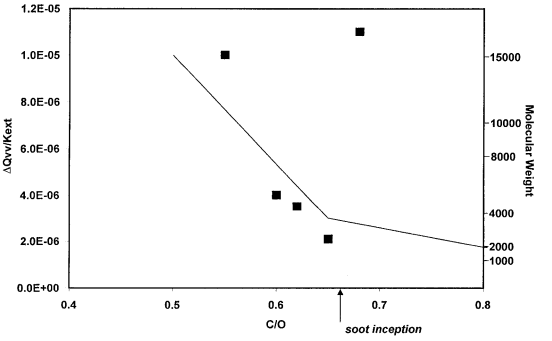

Fig. 5. Comparison between experimental (symbols) [14] and computed excess scattering/extinction ratio at 2.5 mm above the burner of rich ethylene/oxygen flames with C/O ranging from values near the stochiometric one up to very fuel-rich conditions.

ing values but it does not predict the strong increase of scattering in the C/O = 0.77 flame when the inception of soot particles and their coagulation take place since these processes are not included in the model. Figure 4 reports, also as a dashed line, the scattering evaluated when the molecular weight growth process is not included in our calculations for the C/O = 0.77 flame. It is evident that PAHs predicted by the gas-phase model cannot account for the measured scattering in the absence of the radical-molecule reactions leading to the molecular weight growth. The good agreement of model predictions with the experimental results indicates that the proposed kinetic model for aromatic formation and growth is able to predict not only the total amount of particulate matter as measured by absorption (Fig. 3) but also its size distribution (Fig. 4) as measured by scattering.

An estimation of the extent of the molecular growth process of aromatics can be obtained by considering the ratio between scattering and extinction measurements. Indeed, the scattering is proportional to the square of the molar refractivity of nanoparticles whereas the extinction is directly proportional to their molar absorption coefficient. In our approximation, the molar refractivity of nanoparticles is the refractivity of 2-, 3-ring PAHs times the number of subunits inside the nanoparticles whereas the absorption coefficient is the absorption of 2-, 3-ring PAHs times the number of subunits. Thus, the ratio between scattering and extinction is proportional to the number of subunits inside the nanoparticles from which their molecular mass can be retrieved independently on the estimation of the total concentration of the species.

The effect of the different C/O ratio on the molecular growth process has been studied by comparing the measured and predicted scattering/extinction ratios at a fixed height (2.5 mm) of ethylene/oxygen flames for a wide range of C/O ratios [14]. Figure 5 reports such comparison. The model reproduces the experimental data up to soot inception and predicts that the size of the nanoparticles approaches a lower limit as the C/O ratio increases. In particular, the model predicts a molecular weight of the order of 10000 amu (size of 3.2 nm) for the 0.55 flame which decreases steeply to values of the order of about 2000 amu (1.9 nm) before soot inception. Even the radical-molecule molecular weight growth process predicts particles with masses around 1000 amu (1.5 nm) in very fuel-rich conditions.

The formation of large particles in rich flames with C/O just above the stoichiometric value is explained by the high concentration of H-atoms. In fact, although the concentrations of 2-, 3-ring aromatics is low, the high value of H-atoms activates the initiation step of the radical-molecule reactions resulting in structures of high molecular mass. The net rate of the molecular weight growth decreases as the C/O ratio increases since the concentration of H-atoms decreases, even though the concentration of gas-phase aromatics increases. Consequently, structures with low molecular mass are formed.

Aromatics formed under very rich conditions remain in the gas-phase as 2-, 3-ring PAHs instead of being embedded in high molecular mass structures. By contrast, at low C/O ratios, most of the gas-phase PAH are predicted to be in the chain aggregates formed by the radical-molecule reactions. This result can explain the large variation of the percentage of PAH identified in tarry material sampled along flames with different C/O ratios. In fact, the percentage of tarry material that can be separated as GC-chromatographable PAHs in a ethylene/oxygen flame with C/O = 0.5 is about 5% and increases to values as high as 20- to 25% in flames with C/O = 0.8 [28, 35].

DISCUSSION

Previous studies considered PAH growth beyond 4-rings to occur through reactive coagulation models. Frenklach and Wang [36] treated the coagulation process, starting from pyrene, in the free molecular regime considering the coagulation reactions as irreversible having sticking coefficients of unity. A size independent enhancement factor of 2.2 was used in calculations of collision frequencies. Howard [30] described the formation of reactive radical sites in PAH molecules as a result of H atom abstraction. These sites provided a chemical basis for reactive coagulation of PAH compounds with each other and with small radicals.

The model proposed here add chemical specificity to the reactive coagulation process considering radical-molecule sequence of reactions involving gas-phase PAHs having conjugated double bond. The radical species attacks the π bond starting the propagation reaction. Aromatic species are usually considered to give substitution reactions, but there are some compounds which have double bonds that can be easily broken, giving addition reactions, that is, 9,10 bond in phenanthrene [29, 37, 38] and the double bond in the five-membered ring such as acenaphthylene [29]. These double bonds may give addition reactions forming intermediate species in which the electron can migrate all over the structure. The addition step ($Rx2$) produces resonantly stabilized radical intermediates that continue the addition sequence forming higher molecular mass species. There is a substantial decrease in both entropy and enthalpy associated with this reaction. In the molecular weight growth step a C–C bond is formed (phenyl-like) and the non-aromatic double bond of a five-membered ring is broken. With the addition of the energy relieved by the five-membered structure the decrease in enthalpy is rather substantial. The enthalpy dominates at low temperatures, but at high temperatures the entropy contribution increases the importance of the reverse reaction. Therefore, future extensions of the model are necessary to include considerations on the reverse step considering specific molecules.

Recently, Violi et al. [39] have quantitatively analyzed a simple example of such a reaction using quantum chemical approach. Their calculations showed that the addition of aromatic radicals to the π bond of a five-membered aromatic structure occurs without encountering a barrier because the potential energy surface has an attractive character. This result supports the assumption that radical-molecule reactions are suitable to model the growth of aromatics. Furthermore, they suggested that at high H-atom concentrations, the abstraction of an H-atom from the intermediate structure formed by radical-molecule addition gives back a double bond in the five-membered ring thus favoring the termination of the polymerization chain. Inclusion of such reactions will greatly increase computational effort and are planned in the future.

Although uncertainties in the kinetic parameters, the model proposed has the merit to explaining a number of interesting behaviors of rich flames not previously modeled. It interprets the light scattering measured in flames before soot inception and explains quantitatively the formation of very small nanoparticles for which there was only experimental evidences.

The model also allows the formation of high molecular mass aromatics having high H/C ratios and few condensed rings connected by aliphatic bonds. The presence of these compounds has been experimentally found in premixed [14, 40] and diffusion flames [41, 42] and it cannot be explained considering only a growth process of sequential addition of acetylene to aromatic rings.

Rich flames below the soot threshold around the stoichiometric value produce nanoparticles with sizes larger than those produced in slightly sooting conditions. Obviously their amount, which depends on the PAH monomer concentration, is accordingly lower. More interestingly, it shows clearly the role of the H atom concentration in addition to that of PAH chemistry in the formation of nanoparticles.

Experimentally, it should be interesting to explore more systematically premixed flame conditions, starting from the stoichiometric value and moving towards richer mixtures to assess whether the size (or molecular mass) of cross-linked PAHs passes through a maximum. At the same time, more sophisticated diagnostics, like depolarized light scattering, broadening diffusion spectroscopy and microscopy, should be employed to infer information on the chemical nature and morphology of these structures.

The analysis reported in this paper predicts that at larger C/O ratios, where the concentration of H-atoms is lower, the formation of nanoparticles through a radical-molecule mechanism is less efficient. This effect should be even more evident in non-premixed combustion systems, where the pyrolysis of the fuel is almost decoupled from the oxidation chemistry. Experimental and modeling work which is currently running on laminar counterflow diffusion flames should give more information on this issue in the near future. The implications of these considerations are that regimes of nearly stoichiometric or slightly sooting premixed combustion are dominated by reactions different to those that are controlling in fully sooting or diffusion flames, where the fuel-air mixing is not very efficient.

Modern technology of gasoline and diesel engines as well as gas turbines is just moving toward regimes of premixed combustion, giving more emphasis than in traditional engines to the formation of particles in the pre-sooting regime. However, the peculiar chemistry of these regimes should be object of serious considerations to avoid the shift of the pollution problem from a visible particulate (soot particles) to a more unpredictable one (visible-transparent nanoparticles), which may not improve significantly the health impact of combustor particulate emissions.

CONCLUDING COMMENTS

Several groups have proposed polymerization mechanisms in parallel with the HACA mechanism to explain soot growth. The concept in this paper of the linking of 2-, 3-aromatic rings in open structures that grow to yield nanoparticles that subsequently dehydrogenate to form soot adds the ability to explain the following experimental observations:

- H/C ratios. The open structure provides an explanation for the H/C ratios of soot precursors and young soots being greatly higher than those of polybenzenoid structures of equal molecular weight [43].
- Optical properties. The present model explains the decrease with increasing C/O ratio in the size of the particles in the nano-size range. The model also explains why the trends in UV absorption and scatter with increasing residence time, because the open structures formed will not change the absorption characteristics, before dehydrogenation, but will impact the scatter [8, 15].
- Laser Microprobe Mass Spectrometry (LMMS) analysis. LMMS analyses of young soots yield fragments with carbon numbers of 16 to 36 (peak 20 or 22) that correspond to 2-, 3-ring aromatic compounds or their dimers, which might be produced by laser microprobe breaking some of the cross-links [42].
- NMR analyses. NMR measurement of young soots and their precursors formed by the injection of anthracene and pyrene in flames show open structures similar to those proposed in the present study [44].

This research is funded by the University of Naples "Federico II", Department of Chemical Engineering and the University of Utah Center for the Simulation of Accidental Fires and Explosions (C-SAFE), funded by the Department of Energy, Lawrence Livermore National Laboratory, under subcontract B341493.

REFERENCES

1. Schwartz, J., *Environ. Res*. 64:36 (1994).
2. Hannigan M. P., Cass G. R., Lafleur, A. L., Longwell, J. P., and Thilly, W. G., *Environ. Sci. Technol*. 28:2014 (1994).
3. Peters, A., Wichmann, H. E., Tuch, T., Heinrich, J., and Heyder, J., *Am. J. Respir. Crit. Care Med*. 155:1376 (1997).
4. Oberdorster, G., Gelein, R. M., Ferin, J., and Weiss, B., *Inhalation Toxicology* 7:111 (1995).
5. Lighty, J. S., Veranth, J. M., and Sarofim, A. F., *J. Air Waste Manage. Assoc*. 50:1565 (2000).
6. Mayer, A. (Ed.), *Third International Workshop on Nanoparticles*, Zurich, Switzerland, August 9–10, 1999.
7. Wersborg, B. L., Howard, J. B., and Williams, G. C., *Proc. Combust. Inst*. 14:929 (1973).
8. D'Alessio, A., D'Anna, A., Gambi, G., and Minutolo, P., *J. Aerosol Sci*. 29:397 (1998).
9. Bockhorn, H., Fetting, F., and Heddrich, A., *Proc. Combust. Inst*. 21:101 (1986).
10. Woiki, D., Giesen, A., and Roth, P., *Proc. Combust. Inst*. 28:2531 (2000).
11. Hepp, H., and Siegman, K., *Combust. Flame* 115:275 (1998).
12. Shi, J. P., Evans, D. E., Khan, A. A., and Harrison, R. M., *Atmospheric Environ*. 35:1193 (2001).
13. Hall, D. E., Stradling, R. J., Zemroch, P. J., Rickeard, D. J., Mann, N., Heinze, P., Martini, G., Hagemann, R., Rantanen, L., and Szendefi, J., *SAE Paper No*. 2000-01-2000, Warrendale, PA: Society of Automotive Engineering.
14. D'Alessio, A., D'Anna, A., D'Orsi, A., Minutolo, P., Barbella, R., and Ciajolo, A., *Proc. Combust. Inst*. 24:973 (1992).
15. Minutolo, P., Gambi, G., and D'Alessio, A., *Proc. Combust. Inst*. 27:1461 (1998).
16. Ciajolo, A., D'Anna, A., Barbella, R., Tregrossi, A., Violi, A., *Proc. Combust. Inst*. 26:2327 (1996).
17. D'Alessio, A., D'Anna, A., Minutolo, P., Sgro, L. A., and Violi, A., *Proc. Combust. Inst*. 28:1241 (2000).
18. Frenklach, M., and Wang, H., in *Soot Formation in Combustion*, (H. Bockhorn, Ed.), Springer–Verlag, Heidelberg, 1994, p. 165.
19. Frenklach, M., and Wang, H., *Proc. Combust. Inst*. 23:1559 (1990).
20. Wang, H., and Frenklach, M., *Combust. Flame* 110:173 (1997).
21. Marinov, N. M., Pitz, W. J., Westbrook, C. K., Castaldi, M. J., and Senkan, S. M., *Combust. Sci. Technol*. 116–117:211 (1996).
22. Castaldi, M. J., Marinov, N. M., Melius, C. F., Huang, J., Senkan, S. M., Pitz, W. J., and Westbrook, C. K., *Proc. Combust. Inst*. 26:693 (1996).
23. D'Anna, A., and Violi, A., *Proc. Combust. Inst*. 27:425 (1998).
24. Violi, A., D'Anna, A., and D'Alessio, A., *Chem. Eng. Sci*. 54:3433 (1999).
25. D'Anna, A., Violi, A., and D'Alessio, A., *Combust. Flame* 121:418 (2000).
26. Minutolo, P., Gambi, G., D'Alessio, A., and Carlucci, S., *Atmospheric Environment* 33:2725 (1999).
27. Lafleur, A. L., Howard, J. B., Plummer, E., Taghizadeh, K., Necula, A., Scott, L. T., and Swallow, K. C., *Polycyclic Aromat. Compd*. 12(4), 223 (1998).
28. Ciajolo, A., D'Anna, A., Barbella, R., and Tregrossi, A., *Proc. Combust. Inst*. 25:679 (1994).
29. Badger, G. M., *Aromatic Character and Aromaticity*, Cambridge University Press, Cambridge, 1969.
30. Howard, J. B., *Proc. Combust. Inst*. 23:1107 (1990).
31. Kee, R. J., Rupley, F. M., and Miller, J. A., (1989), Chemkin II: A Fortran Chemical Kinetics Package for the analysis of gas phase chemical kinetics, *Sandia National Laboratories Report No. SAND 89-8009B*.
32. Homann, H. K., in *Soot Formation in Combustion. An International Round Table Discussion*, H. Jander & H. Gg. Wagner (Eds.), Vandenhoeck & Ruprecht, Gottingen, 1990, p. 101.
33. Gardiner, W. C., Hidaka, Y., and Tanzawa, T., *Combust. Flame* 40:213 (1981).
34. Harris, S. J., in *Soot Formation in Combustion. An International Round Table Discussion*, H. Jander & H. Gg. Wagner (Eds.), Vandenhoeck & Ruprecht, Gottingen, 1990, p. 101.
35. Barbella, R., Ciajolo, A., D'Anna, A., and Tregrossi, A., CROCUS '94, Salsomaggiore, Italy, paper no. III-13, 1994.
36. Frenklach, M., and Wang, H., *Proc. Combust. Inst*. 23:1559 (1990).
37. Clar, E., *The Aromatic Sextet*, John Wiley & Sons, New York, 1972.
38. Garratt, P. J., *Aromaticity*, John Wiley & Sons, New York, 1986.
39. Violi, A., Truong, T. N., and Sarofim, A. F., Quantum Mechanical Study of Molecular Weight Growth Process, *Combust. Flame* 126:1506 (2001).
40. Ciajolo, A., Barbella, R., Tregrossi, A., and Bonfanti, L., *Proc. Combust. Inst*. 27:1481 (1998).
41. Dobbins, R. A., and Subramaniasivam, H., in *Soot Formation in Combustion*, (H. Bockhorn, Ed.), Springer–Verlag, Heidelberg, 1994, p. 290.
42. Dobbins, R. A., Fletcher, R. A., and Chang, H.-C., *Combust. Flame* 115:285 (1998).
43. Keller, A., Kovacs, R., and Homann, K.-H., *Phys. Chem. Chem. Phys*. 2:1667 (2000).
44. Solum, M. S., Sarofim, A. F., Pugmire, R. J., Fletcher, T., and Zhang, H., *Energy & Fuels* 15:961 (2001).

Received 26 January 2001; revised 5 June 2001; accepted 16 July 2001